Experimental and numerical investigation on the role of interface for crack-width control of hybrid SHCC concrete beams

Mustafa, S.; Singh, S.; Hordijk, D.; Schlangen, E.; Lukovic, M.

DOI
10.1016/j.engstruct.2021.113378

Publication date
2022

Document Version
Final published version

Published in
Engineering Structures

Engineering Structures 251 (2022) 113378

Contents lists available at ScienceDirect

Engineering Structures

journal homepage: www.elsevier.com/locate/engstruct

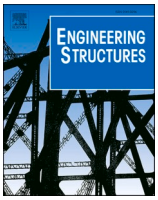

Experimental and numerical investigation on the role of interface for crack-width control of hybrid SHCC concrete beams

Shozab Mustafa [a,*], Shantanu Singh [a], Dick Hordijk [b], Erik Schlangen [c], Mladena Luković [a]

[a] Concrete Structures, Delft University of Technology, Delft, the Netherlands
[b] Adviesbureau ir. J.G. Hageman B.V., the Netherlands
[c] Materials and Environment, Delft University of Technology, the Netherlands

ARTICLE INFO

Keywords:
Hybrid Reinforced SHCC Concrete Beams
Interface
SHCC
Cracking
Lattice Modelling

ABSTRACT

Hybrid application of conventional concrete and Strain Hardening Cementitious Composite (SHCC) is recently shown to be promising for crack width control. In this paper, a combined experimental and numerical study is performed to validate the concept and to study the effect of interface treatment on crack width control. The interface is varied between smooth, profiled, partially debonded and completely debonded surfaces. The beams are tested under a four-point bending configuration. The crack development is monitored using digital image correlation throughout the loading, and maximum crack width of 0.3 mm at the surface is taken as the limiting criterion for analyses. The hybrid and control beams are simulated using the lattice model. Both experimentally and numerically, it is observed that stronger interfaces enable the composite action in the hybrid beams and provide better crack width control compared to the artificially weakened interfaces.

1. Introduction

Concrete is the most commonly used construction material in the world due to, among others, its high compressive strength and the ease to be cast in various shapes. Under uniaxial tensile loads, concrete has low strength and shows a brittle strain-softening behaviour [1] with the formation of a single localized crack leading to failure. Therefore, concrete structures are generally reinforced using steel reinforcement to create capacity i.e., to sustain design tensile loads (Ultimate Limit State, ULS). Given that the reinforcement should be protected for durability, it is necessary to limit the surface crack widths in concrete under serviceability conditions (Serviceability Limit State, SLS), such that the ingress of deleterious substances is limited and the durability of concrete structure is ensured. In many structural applications, the criterion for crack width control is governing and leads to additional reinforcement than required to sustain the design loads. Such reinforcement, though required for crack width control, does not contribute to structural capacity, making the design uneconomical.

In recent decades, a new type of fibre reinforced concrete has been developed, showing strain-hardening response under uniaxial tensile loads [2]. It is referred to as Strain Hardening Cementitious Composite (SHCC). The strain hardening ability of SHCC is achieved by engineered micromechanical design [3]. This design allows SHCC to develop multiple cracks (microscopic cracks with width < 100 μm) and a, by two orders of magnitude, larger ductility compared to that of the conventional concrete. Some researches [4] show that reinforced SHCC also exhibits improved durability when compared to the conventional reinforced concrete. However, the complete replacement of conventional reinforced concrete with reinforced SHCC is, among others, not a cost-effective solution due to the higher material cost of SHCC.

An optimal solution can possibly be achieved by applying SHCC and conventional concrete in combination where SHCC is only used at locations in the structures where needed, like the tension side of a flexural member to limit crack widths. Several studies have investigated the effectiveness of SHCC concrete hybrid systems for different structural members, for example shear strengthening by placing SHCC on sides of a beam [5,6] and flexural strengthening by placing SHCC at the tension side [7]. An overview of strengthening applications can be seen in [8]. These studies, along with the study on new hybrid system [9], demonstrate the promising application of hybrid structures by highlighting the increase in load-carrying capacity. However, little attention is paid to the maximum crack widths and the properties of the interface between the two types of concrete, while they may govern the behaviour of such hybrid systems, both in SLS and ULS. In a recent study [10], the crack

* Corresponding author.
E-mail address: s.mustafa-2@tudelft.nl (S. Mustafa).

https://doi.org/10.1016/j.engstruct.2021.113378
Received 28 June 2021; Received in revised form 22 September 2021; Accepted 12 October 2021
Available online 10 November 2021

width control ability of hybrid SHCC concrete beams, with reinforcement embedded in SHCC, is investigated. It is reported that providing a 70 mm thick layer of SHCC in the tensile zone of a 200 mm beam eliminates the crack width control as governing design parameter. However, the study is limited to one type of interface preparation between SHCC and the conventional concrete.

Embedding the reinforcement in SHCC allows the reinforcement to be activated in tension while the cracks around it remain small, so the reinforcement is sufficiently protected. However, in hybrid systems, the SHCC layer is also restrained along one edge (interface with the concrete), and therefore, the straining behaviour of SHCC is not possible at that edge. If a crack occurs in the conventional concrete, the same crack width will tend to reflect (occur) in SHCC directly adjacent to the interface. The effect of this interfacial boundary condition on the crack width control ability of SHCC with embedded reinforcement is still unknown. Current design codes and standards provide limited information for the safe design of hybrid structures, especially the design calculation of the interface. The mean roughness of the interface profile is commonly used to estimate the interface strength [11,12]. Although the effect of interfacial treatment is well recognised for strength of the interface [11,13,14], little has been reported on its influence on crack width control in hybrid systems.

The effect of interface treatment on crack width control has been studied for repair applications [15–17] where SHCC is applied on pre-cracked concrete surfaces. The studies conclude that a weak interface (represented by smooth profile, or local debonding) is beneficial for crack width control because a larger portion of SHCC is activated around the pre-existing crack in concrete resulting in improved ductility of the repair system. Contrarily, a strong interface resists the debonding and causes earlier localization of cracks in SHCC (see Fig. 1).

In the current study, the role of the interface treatment on the cracking behaviour of hybrid SHCC concrete systems is investigated. The starting hypothesis is that a weaker interface would cause more cracks with smaller crack widths in SHCC, and hence provide a better crack width control. Since the cracking behaviour of SHCC depends on the fibres incorporated in the mix [18], two of the most commonly used SHCC fibre types are used: Polyvinyl Alcohol (PVA) and High Modulus Polyethylene (HMPE).

The need for developing reliable models for structural interfaces and advanced modelling of hybrid concrete structures, and the complexity of obtaining reliable interface behaviour are widely recognized [19,20]. In this study, an attempt is made to use a simple fracture model – a discrete type lattice model – in which interface is defined using fundamental parameters (i.e. tensile/compressive strength and elastic modulus) to acquire advance insight into the physical phenomena occurring at the interface, and determine the governing parameters and their role on the behaviour of the hybrid systems.

1.1. Research significance

This study investigates the effect of interface treatment between SHCC and concrete on the crack width development in SHCC concrete hybrid beams and highlights the potentials and limitations of lattice modelling to simulate such structures. The role of different fibres in SHCC is also studied. The knowledge gained will provide an insight into the optimal design of hybrid SHCC concrete structures where SHCC is applied for crack-width control.

2. Experimental methods

2.1. Experimental design

The test program consists of six beams including one traditional reinforced concrete beam as a reference sample. Four hybrid beams are made with 70 mm thick SHCC layer containing PVA fibres and embedded reinforcement. As the crack width development is studied in the constant moment region of the beam (central 500 mm in Fig. 2), the interface treatment is ensured in this region. The interface is varied between smooth, profiled, partially debonded and completely debonded surfaces. The longitudinal and cross sections of the beams are shown in Fig. 2. The profiled beam is intended to represent the strongest interface due to the mechanical interlock between the grooves while the completely debonded interface represents the other extreme where no composite action is realized between SHCC and concrete. The smooth and partially debonded beams are intended to represent intermediary behaviour. Additionally, a hybrid beam with a smooth interface is cast with HMPE fibres to study the effect of varying the fibre type. PVA fibres are well known for their hydrophilic nature and their ability to form a strong chemical bond with the matrix. Therefore, significant energy is required to break the fibre–matrix adhesion bond for slippage of the fibres to occur: this can reduce the ductility of SHCC due to early rupture of the fibres. To avoid this, the PVA fibres used in this study were surface treated with oil by the producer to reduce the fibre–matrix bond and to have better dispersion in the cement matrix. HMPE fibres, on the other hand, have a hydrophobic nature (weaker adhesion bond) and are approximately two times as strong as PVA fibres in tension. HMPE fibres provide fibre bridging predominantly due to the friction caused by fibre slippage which, combined with their higher strength, leads to higher ductility compared to SHCC with PVA fibres [18].

The reference beam is referred to as Reinforced Concrete, and the hybrid beams with the smooth interface are referred to as Smooth(PVA) or Smooth(HMPE), depending on the fibres incorporated in SHCC. The rest of the hybrid beams contain PVA fibres and are distinguished based on the interfacial treatment. These are referred to as Profiled, Partial Debond and Complete Debond, and are schematically represented in Fig. 2.

The specimen geometry from the preliminary study [10] is adopted. All the beams have identical geometries of 1900 mm length, 150 mm width and 200 mm height. For the hybrid beams, the bottom 70 mm of concrete is replaced with SHCC. Beams have the same reinforcement configuration with 3 −Φ8 ribbed rebars at the bottom and 2 −Φ8 ribbed rebars at the top (see the cross section in Fig. 2). The percentage of

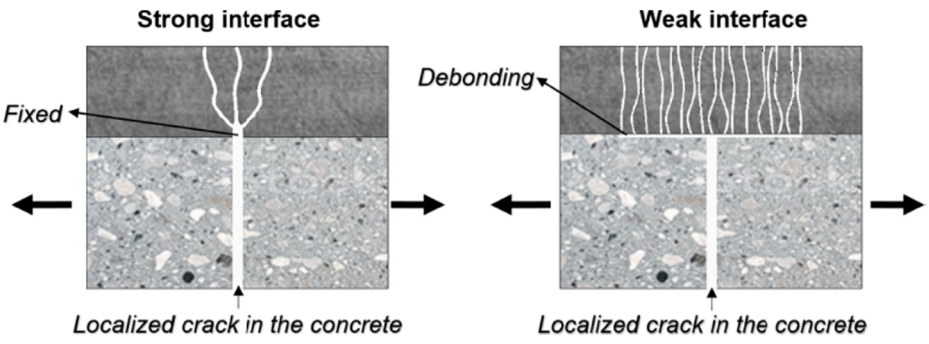

Fig. 1. Distribution of a pre-existing crack in concrete to SHCC for repair applications.

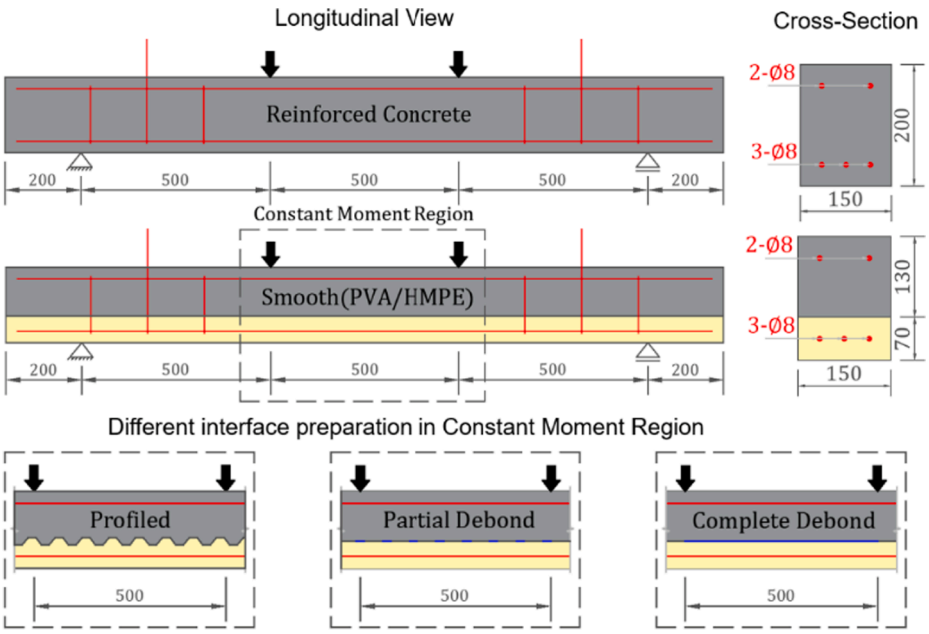

Fig. 2. Longitudinal and cross sections of the reference and hybrid beams with varying treatment of interface within the constant moment region. Concrete (Grey), SHCC (Yellow), Rebar (Red) and Debond (Blue). All dimensions are in mm.

longitudinal reinforcement is kept close to the minimum to allow for large crack widths to develop in the constant moment region of the reference beam. To ensure that the beams fail in flexure, the stirrups of Φ8@150 are provided in the shear span. The central stirrup on both sides is extended upward such that it is protruding out of the beam to help in the handling of the samples.

2.2. Materials, specimen preparation and casting

All the hybrid beams are cast in two phases. In the first phase, the reinforcement cage is placed in plywood moulds using spacers, and the 70 mm thick layer of SHCC is poured. This layer is then compacted using a vibrating table. For smooth interface, the surface is levelled with a trowel immediately after compaction, and for profiled surface, a plastic sheet with 18 mm grooves at a distance of 70 mm is pressed onto the freshly cast SHCC and held in place using small weights. The beams are then cured in sealed condition for 14 days to allow SHCC to shrink before casting the concrete layer. The surface preparation for the completely debonded and partially debonded beams is performed after the hardening of the SHCC. For the partially debonded interface, a tape with 20 mm width is placed at a distance of 70 mm, while for the completely debonded interface, it is placed throughout the constant moment region. Fig. 3 provides a pictorial representation of all the interfaces before casting the concrete layer. The SHCC top surfaces are cleaned using an air jet, wire brush and ethanol to ensure no dust at the interface before casting the concrete layer. After surface preparation and cleaning, the second phase of casting is performed where the top layer of concrete is cast and compacted using a vibration needle. The hybrid beams are then cured for 38 days in sealed conditions before testing. Reinforced Concrete (reference beam) is cast along with this second phase, so the concrete has the same age in all the tested beams.

A fixed fibre volume fraction of 2% is used for SHCC irrespective of the fibre type. The properties of PVA and HMPE fibres are listed in Table 1, and Table 2 provides the mix composition of SHCC and concrete. The SHCC mix used in this study is developed at TU Delft [21] in efforts to produce green SHCC by using locally available materials in the Netherlands.

In parallel to making hybrid beams, SHCC samples with PVA and

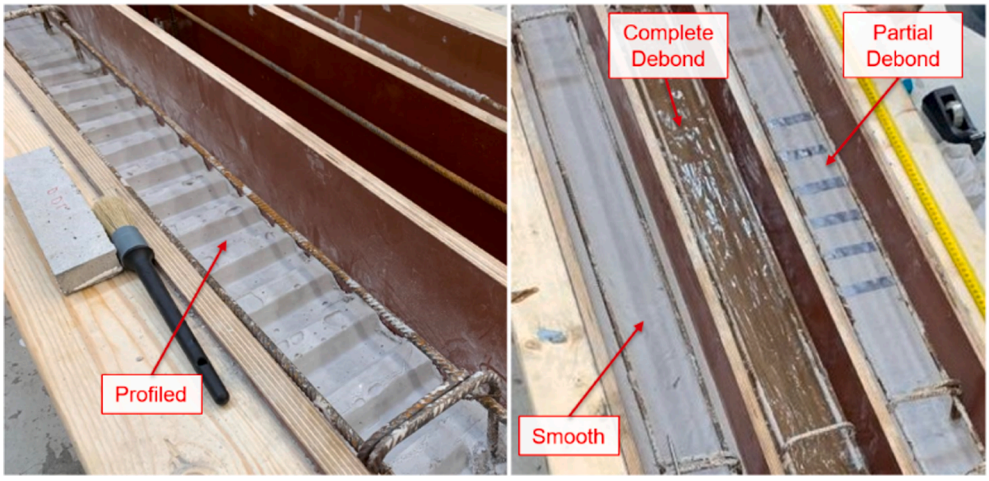

Fig. 3. Interface preparation of the hybrid beams before casting the concrete top layer.

Table 1
Properties of the fibres used in SHCC.

Property	PVA	HMPE
Tensile Strength (MPa)	1640	3400
Young's Modulus (MPa)	41,100	113,000
Density (kg/m^3)	1300	970
Diameter (mm)	0.04	0.02
Length (mm)	8	6

Table 2
Mix composition of concrete and SHCC [21].

Material (amount in kg/m^3)	SHCC (PVA)	SHCC (HMPE)	Concrete
CEM IIIB	790	790	–
CEM I 52.5 R	–	–	260
Limestone Powder	790	790	–
Sand (0.125–4 mm)	–	–	847
Gravel (4–16 mm)	–	–	1123
Fibres	26	19.4	–
Water	411	411	156
Superplasticizer	2.13	2.13	0.26

HMPE fibres are created for material testing. Specimens of dimensions 30 mm × 8 mm × 180 mm are cast and left to cure in sealed conditions for 14 days. The specimens (4 for each fibre type) are then tested in a four-point flexural tests using a displacement controlled analysis at a loading rate of 0.01 mm/sec (Fig. 4a). To determine the compressive strength of concrete, 150 mm × 150 mm × 150 mm cubes are cast with each casting phase of the beams, and are tested following NEN-EN 12390-3 [22].

2.3. Structural testing and monitoring

All the beams are tested under a four-point bending test configuration as schematized in Fig. 2 and shown in Fig. 4b. A displacement-controlled procedure is adopted for loading the specimens at a rate of 0.01 mm/sec. The deformation of the beams is measured in the constant moment region using Linear Variable Differential Transformers (LVDTs) on one side of the beam and Digital Image Correlation (DIC) on the other, see Fig. 4b. DIC is a non-contact optical technique that tracks pixel movements in images at varying deformation levels to provide full-field deformations and strains [23]. The beam surface is prepared for DIC by first painting a white layer over which a black speckle pattern is created using a roller brush. Images are captured throughout the loading with every 5 kN increase in the applied load. A single camera is used, as only in-plane deformations of the beam are of interest. The crack widths are measured using DIC and visual observation using a microscope. The results of the DIC have a crack width measurement resolution of 0.025 mm and the crack widths are verified by comparing them with the LVDT measurements, microscope measurements and photographs analysed by image processing software ImageJ [24]. These verification results and a brief account of the experimental process are reported in [10,25].

3. Experimental results

3.1. Material properties

Based on four-point bending material tests on SHCC, samples containing HMPE fibres exhibited higher deformation capacity than the samples containing PVA fibres. The results are summarised in Fig. 5a, which shows the bending stress (assuming linear elastic stress distribution) against the mid-span deflection of the samples. The larger ductility with HMPE fibres is due to weaker fibre–matrix adhesion bond and larger frictional resistance at fibre–matrix interface leading to more cracks. From the deflection hardening curve, it can be seen that the cracking stress of matrix is comparable for both the fibre types but the ultimate strength of SHCC with HMPE fibres is higher due to higher tensile strength of the fibres. Although the SHCC with HMPE fibres shows enhanced deformation hardening, the scatter in results of the samples with HMPE fibres is larger when compared to the samples with PVA fibres. The next step is to investigate the role of these fibres on structural behaviour and crack development in the hybrid beams, where cracking behaviour of SHCC is also influenced by the embedded steel reinforcement, restraint at the interface and cracking in the adjacent concrete.

The average compressive strength of concrete measured at the day of testing of the beams is 49.4 ± 2.2 MPa which is in line with the previously measured value of 46 MPa [10]. The average compressive strength of SHCC is found to be 49.3 ± 5.3 MPa.

3.2. Structural behaviour

In the structural tests and analyses, for the load deformation relation and crack width response, a comparison is made between the reference (Reinforced Concrete) beam and the hybrid beams. Special attention is paid to the crack development, crack pattern and the ability of the beams to limit the maximum crack width to be lower than the SLS criterion. For this paper, a maximum crack width of 0.3 mm at the surface is taken as the limit – this value is recommended for reinforced concrete under quasi-permanent load for all exposure classes except for X0 and

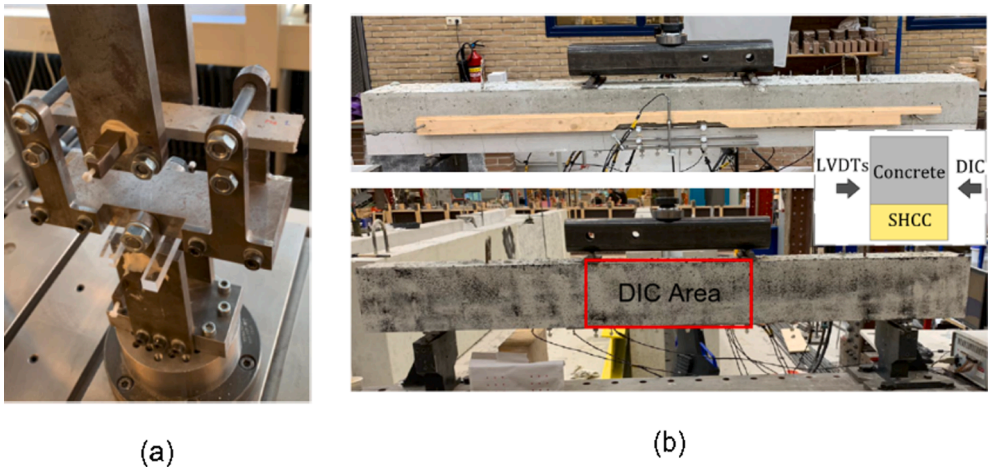

Fig. 4. Test setup for (a) material tests for the effect of fibre types in SHCC and (b) structural tests with LVDT measurement on one side and DIC on the other. DIC results discussed in this paper correspond to the constant moment region of the beam, as demarcated in red.

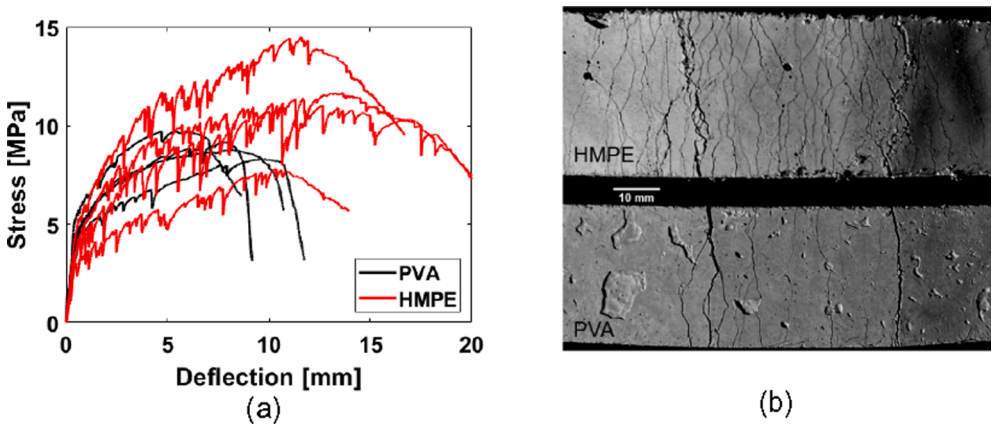

Fig. 5. (a) Bending stress assuming linear elastic stress distribution against mid-span deflection of SHCC with PVA and HMPE fibres and (b) cracks after failure of a typical HMPE and PVA sample.

XC1 in Eurocode 2 [12].

3.2.1. *Verification of the previous study*

Firstly, a comparison is made between the reference (Reinforced Concrete) beam and hybrid beam with smooth interface (Smooth(PVA)). This comparison allows to prove the concept that a better crack width control can be achieved by replacing a part of concrete by SHCC on the tension side of a flexural member. In this comparison the results of the previous study (two hybrid and one reference beam [10]) are used to check the reliability and reproducibility of the experiments. Fig. 6a shows the comparison of load-deformation-crack width response of these beams. The maximum crack width is recorded near the bottom edge of the beam corresponding to the maximum crack in the constant moment region. This can be a different crack in each loading step. These crack widths are calculated using displacement (d_x) along the length of the beam with a strain (ε_{xx}) cut-off to define the crack location, a similar procedure is detailed in [26].

A comparison is made between the load at which the crack width exceeds the 0.3 mm criterion for Reinforced Concrete and Smooth(PVA) for both the studies. It can be seen that the results of Reinforced Concrete are reasonably replicated for both load-deformation capacity and the crack width response. Although the maximum crack width development shows some deviation for the three hybrid beams, for all the beams the maximum crack width exceeds 0.3 mm after the yielding of reinforcement (observed as a kink on the load–deflection curve). For the two hybrid beams from the previous study, the crack width reaches 0.3 mm as soon as the reinforcement yields, whereas in the new beam, the beam is long in the yielding phase before exceeding the 0.3 mm maximum crack width criterion. Due to the fact that the reinforcement yields prior to exceeding the 0.3 mm limit in all the beams, SLS criterion is no longer governing and the loads at which SLS criterion is reached are comparable. This validates that for the investigated configuration, a better crack width control can be achieved when concrete is replaced with SHCC on the tension side of the beam, and ensures the reproducibility of the experiments.

The lower deformation capacity in both, the reference and the hybrid beams reported in Fig. 6a, correspond to the experiments from the previous study where the LVDT measuring the deflection of the beam reached its capacity. Therefore, the lower deformation capacity is not because the beam failed prematurely but because of the limitation of measuring device. This limitation does not affect the results of the study because the 0.3 mm crack width criterion is exceeded within the measured range.

3.2.2. *Role of fibres*

Comparing the results of Smooth(PVA) and Smooth(HMPE) in Fig. 6b, it can be seen that Smooth(HMPE) did not perform better in the structural test and exhibited a similar crack width control ability as the Smooth(PVA). In both cases, the maximum cracks at the surface of the SHCC reached the limit of 0.3 mm after yielding of the reinforcement. Once the yielding of the reinforcement is initiated, the increase in maximum crack width at the surface is significantly influenced by the

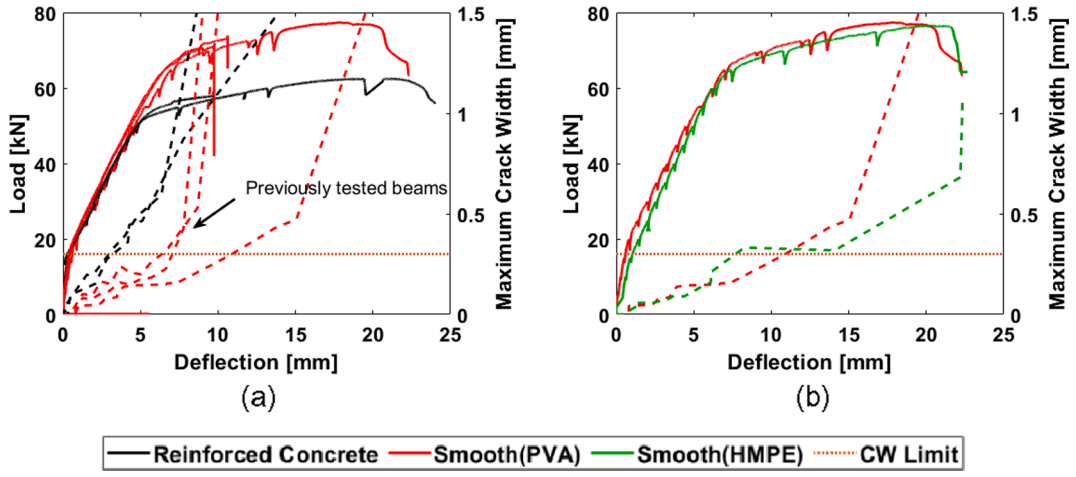

Fig. 6. Load-deflection-crack width response of (a) two reinforced concrete and three hybrid beams with PVA fibres and smooth interface and (b) hybrid beams with varying fibre types. Solid lines represent load–deflection response while dotted lines show the maximum crack widths at the surface of SHCC.

plasticity of rebar and the higher ductility of SHCC with HMPE fibres could not further improve the cracking response of the hybrid beam.

In Fig. 7, the crack pattern at ultimate load of Smooth(PVA) and Smooth(HMPE) is shown. Both the beams show similar load deformation response and the crack width control near the bottom edge of the beam, however, some differences can be seen in the cracking pattern. Smooth(PVA) shows relatively straight cracks in SHCC while the SHCC cracks in Smooth(HMPE) merge towards the localized cracks in concrete. In addition a more distinct debonding of the interface is observed in Smooth(PVA) compared to Smooth(HMPE). These observations indicate that the interface is stronger in Smooth(HMPE) when compared to Smooth(PVA). Still, both the beams effectively limit the cracks to be lower than 0.3 mm until the yielding of reinforcement, after which the plasticity of rebar controls the crack growth.

3.2.3. Role of the interface treatment

A comparison of load deformation response and crack development between the hybrid beams with varying interface treatment is made in Fig. 8. As expected, all the hybrid beams have a similar load carrying capacity due to the stirrups crossing the interface in the shear span. The capacity of the hybrid beams ranges from 73 kN to 78 kN, which is 11–16 kN higher than the capacity of Reinforced Concrete. This increase in capacity is due to the contribution of SHCC in tension, as reported in [10]. More importantly for the aims of this study, it can be observed that the crack widths exceed 0.3 mm in Reinforced Concrete already at the load of 39 kN while the hybrid beams, Smooth(PVA) and Profiled, limit the crack widths until the loads of 71 kN and 69 kN respectively. For both these beams, the cracks in SHCC exceed the 0.3 mm criterion long after the yielding of reinforcement, as also elaborated further in the paper. Complete Debond provides the least crack width control among all the hybrid beams due to lack of monolithic actions between the two concretes and limits the cracks below 0.3 mm only until 44 kN. Partial Debond is able to limit the cracks below 0.3 mm until 54 kN. The crack widths reach the 0.3 mm limit at almost the same deflection in Complete Debond and the Partial Debond, therefore the load in Complete Debond might be lower only due to its less stiff response. Improving the bond between concrete and SHCC from Complete Debond to Partial Debond and from Partial Debond to Smooth(PVA) provides a better crack width control, i.e. crack widths at the surface of SHCC exceed the 0.3 mm limit at higher loads.

For Smooth(PVA) and Profiled, a comparable behaviour is observed. The smooth interface is able to provide enough composite action to fully utilise the crack width control ability of SHCC in the given boundary conditions i.e., the crack width exceed the 0.3 mm limit long after the yielding of the reinforcement (Fig. 8). Further increase in surface roughness did not result in a better crack width control because after yielding the plasticity of rebar controls the crack growth. Therefore, it is emphasized that there are two governing parameters: (1) behaviour of the interface and (2) yielding of the reinforcement. As long as there is no yielding, the interface properties play a crucial role. After yielding of the reinforcement, the plasticity of rebar governs the crack growth.

Fig. 9 shows the DIC results of the constant moment region of Smooth (PVA) and Profiled at 30 kN, 60 kN and ultimate failure load of the beam. For the DIC results, the cracks in SHCC can be appropriately presented by plotting the strain in x-direction. However, then the delamination, which occurs in y-direction, would not be visible. In order to enable visualization of both, the cracks in SHCC and the delamination, equivalent von Mises strains are presented. Although von Mises strains are usually used for ductile materials, the strain concentrations are related to crack formation and as such, these strains are reported to visualize cracks in concrete and masonry [27–29]. Even though the number of cracks in SHCC is similar for both, Smooth(PVA) and Profiled, at all the load levels, the cracking pattern is different. Smooth(PVA) shows the development of relatively straight cracks in SHCC while the SHCC cracks in Profiled tend to merge towards the cracks in concrete as they approach the interface. This difference is due to the additional strength provided by the mechanical interlock of the grooves in profiled surface, which forces the cracks in SHCC to merge at the interface. Comparing the cracks at 60 kN, it can be seen that there are more strain concentrations at the interface for Profiled than for Smooth(PVA). This can be due to the larger dilation of the interface due to the presence of grooves. It is emphasized that the cracks in both the hybrid beams exceed the 0.3 mm limit long after the yielding of the longitudinal reinforcement. This indicates that the benefits of this hybrid system might be even larger for the beams reinforced with a smaller percentage of longitudinal reinforcement and for more practical beam sizes i.e. total height larger than 200 mm. The scale effect and its role on crack control ability of hybrid systems will be further investigated in future.

A similar comparison is made between Partial Debond and Complete Debond as shown in Fig. 10. Although Partial Debond shows little delamination at the load of 30 kN and 60 kN, an obvious opening of the interface is visible in Complete Debond, even at the load of 30 kN. This is because of the lack of bond between the two types of concrete causing both parts of the beam to bend independently, and resulting in the opening and sliding of the interface. This proves that, although a portion of friction might still be present, the desired condition of no bond at the interface is effectively achieved by applying tape over the earlier cast layer of SHCC. In Partial Debond, the cracks in SHCC are relatively straight showing that SHCC and concrete exhibit composite action. Combined with the observations from Smooth(PVA) and Profiled, it can be said that a strong bond between SHCC and concrete ensures that the tensile stresses in SHCC are rather uniform. Contrarily, the cracks in SHCC of Complete Debond seem to close and vanish as they reach the interface because no composite action is activated and SHCC predominantly experiences bending – this is also elaborated further in the paper.

In Partial Debond, seven cracks developed in concrete at ultimate load corresponding to the seven regions where bond is allowed to be formed between concrete and SHCC. However, in Complete Debond only four cracks developed in concrete due to lack of monolithic action. These cracks are caused by the friction between SHCC and concrete, and the stirrups outside the constant moment region.

Comparing the results of Partial Debond and Complete Debond on the one side, with Smooth(PVA) and Profiled on the other side, it can be seen that the former is not able to fully utilize the multiple cracking behaviour of SHCC – this is evident from the lower number and larger spacing of cracks in SHCC at ultimate load. Therefore, unlike in repair

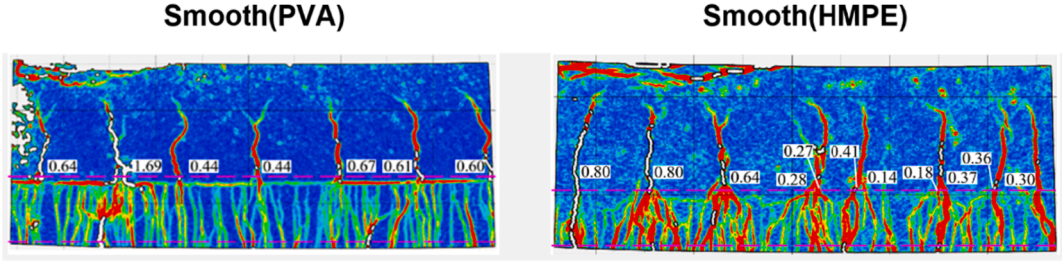

Fig. 7. Crack pattern at ultimate load of hybrid beams with smooth interface and varying fibre types.

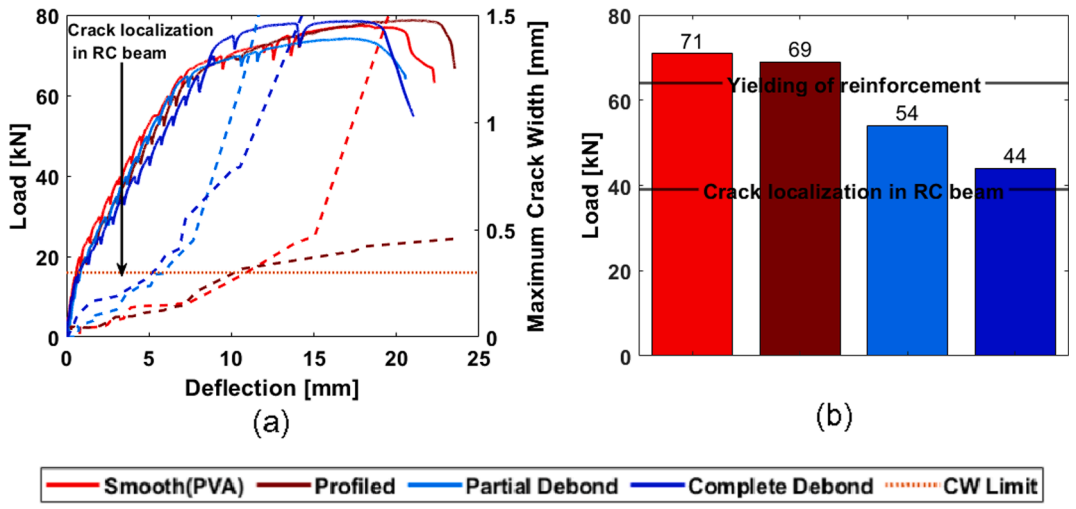

Fig. 8. (a) Load-deflection-crack width response of the four hybrid beams with PVA fibres and varying interface treatment. Solid lines represent load–deflection response while dotted lines show the maximum crack widths near the bottom of the beam. (b) Bar graph of loads at which the crack widths in each hybrid beam exceeds the 0.3 mm limit.

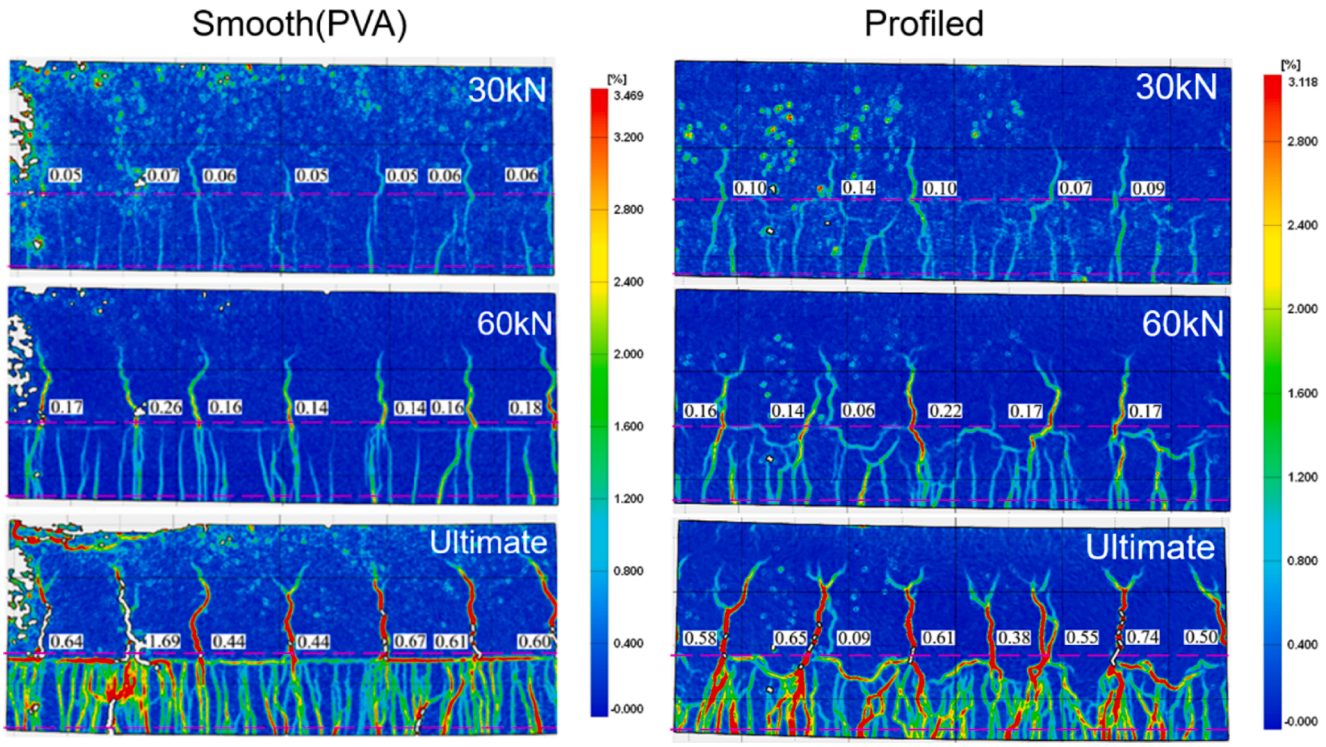

Fig. 9. Development of cracks in constant moment region for Smooth(PVA) and Profiled samples at 30 kN, 60 kN and ultimate load. The dashed horizontal lines show the section where crack widths are measured in SHCC and in concrete.

applications where weaker interfaces provide better crack width control by allowing debonding of the interface around the pre-existing cracks in concrete and activating a larger part of SHCC, in the design application of new hybrid beams a strong interface provides better crack width control. This is because in repair applications the cracks in concrete are created before application of SHCC thus the properties of the interface do not influence the pre-existing crack development in concrete. The interface only plays a role in generating the cracks in SHCC once the pre-existing cracks in concrete tend to increase (e.g. due to imposed load) or SHCC tends to shrink (due to imposed deformations). However, in design applications of new hybrid structure, the development and distribution of cracks in concrete are dependent on the strength of the interface and the properties of SHCC. Weaker interfaces fail to provide the required strength to mobilize the composite action of SHCC and concrete, hence SHCC experiences larger stresses leading to earlier crack localization.

In Fig. 11, the cracks in Smooth(PVA) and Complete Debond are compared at the load of 40 kN and 70 kN i.e. close to the moments when crack widths at the surface of SHCC exceed 0.3 mm in the two beams. Crack widths in concrete are labelled next to the cracks whereas crack widths in SHCC are given via a scatter plot below the cracks. It is observed that the trend of exceeding the 0.3 mm crack width in SHCC is closely related to the development of maximum crack in concrete. Cracks in the concrete at 40 kN are around 3 times larger in Complete

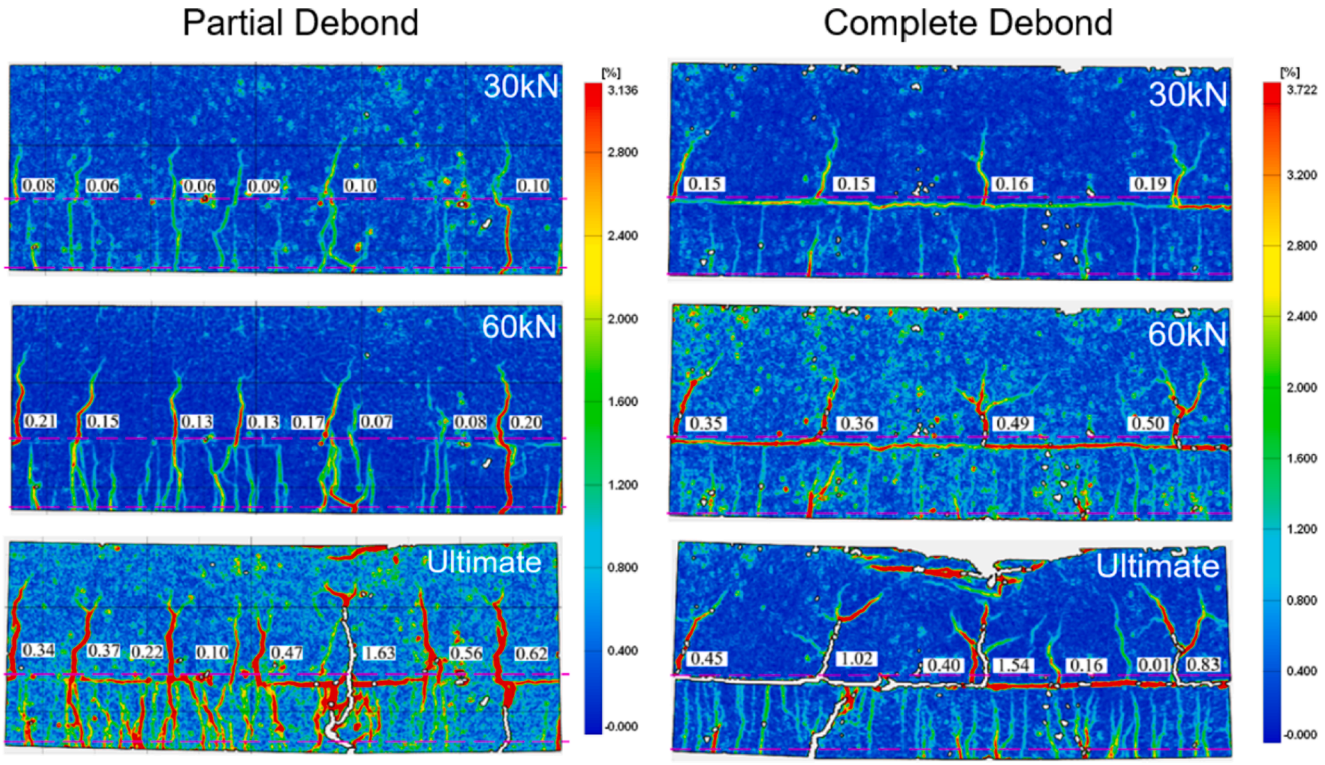

Fig. 10. Development of cracks in the constant moment region of Partial Debond and Complete Debond at 30kN, 60 kN and ultimate load. The dashed horizontal lines show the section where crack widths are measured in SHCC and in concrete.

Debond than in Smooth(PVA), leading to earlier localization of the cracks at the surface of SHCC. Interestingly, cracks in the concrete, for both samples, are of similar magnitude when the maximum cracks in SHCC exceed 0.3 mm. It seems that the crack width in concrete is also governing the crack development in SHCC. The crack width in concrete is determined by the effective reinforcement provided by the SHCC layer. A stronger bond causes a more effective reinforcement of the concrete and therefore provides that the cracks in SHCC exceed the 0.3 mm criterion at a higher load. It is further investigated if the same trend and behaviour can be captured in the numerical study.

4. Numerical analyses

4.1. Introduction

The lattice modelling approach is widely used in material research for simulating fracture, moisture transport and chloride diffusion in cement based systems [30–32]. Only recently there has been some interest in using the lattice modelling approach to simulate the structural behaviour of reinforced concrete [33,34]. These studies present a promising opportunity to explore and understand the fundamental mechanisms in structural members. In this paper, the possibility of using the lattice approach for modelling hybrid concrete structures is investigated. Simulating such structures still presents a challenge using commercially available finite element software due to the (1) complex non-linear behaviour of interface when loaded parallel and perpendicular to its plane and (2) still unknown interaction between these behaviours.

In the original lattice model, the material is discretized using a set of truss or beam elements connected to each other through lattice nodes. The lattice elements are assigned certain properties to model the behaviour of the discretized material. In each load step, a linear elastic computation is performed where the structure is loaded by a certain deformation or load. The stresses in each lattice element are then compared with the assigned element strength and the element having the highest stress/strength ratio is removed from the mesh thereby simulating fracture [31]. Then a new analysis is performed with the removed element and this process is repeated until the ultimate failure of the structure.

For structural application of lattice model, the bond between reinforcement and concrete has to be addressed and for hybrid application, the interface between two materials requires attention. The systematic procedure adopted for these interfaces is explained below and a 2D representation of both is shown in Fig. 12.

- The 3-dimensional volume of the specimen is divided into cubic voxels of equal dimensions (labelled as Voxel in Fig. 12). The choice of the voxel size depends on the modelled specimen size and the limitation of computation power. For all the simulations reported in this study, a voxel size of 10 mm is used.
- Within each voxel, a sub-voxel is defined in which a node can be randomly generated. The size of the sub-voxel depends on the randomness that is specified to the lattice mesh. A randomness of zero means that the node is generated at the centre of the voxel while a randomness of one means that the node can be generated anywhere within the voxel. Assigning certain randomness to the lattice mesh introduces the heterogeneity to the material through irregularities in the mesh geometry. In this work, in order to use the benefits of random mesh but to avoid large variations in element lengths, a randomness of 0.5 is adopted [31].
- Lattice nodes are connected to each other using Delaunay triangulation and the connecting member are referred to as lattice elements. Each lattice element has 6 degrees of freedom on each node and is assigned material properties based on the material it represents.
- For reinforcement, the interface between rebar and concrete is to be simulated. The rebar is added following the geometry of the member and the extra nodes are generated at the edges of all the voxels containing rebar elements. These extra nodes (labelled as rebar nodes) are then connected to the concrete node of the corresponding voxel through the interface elements, see Fig. 12a.

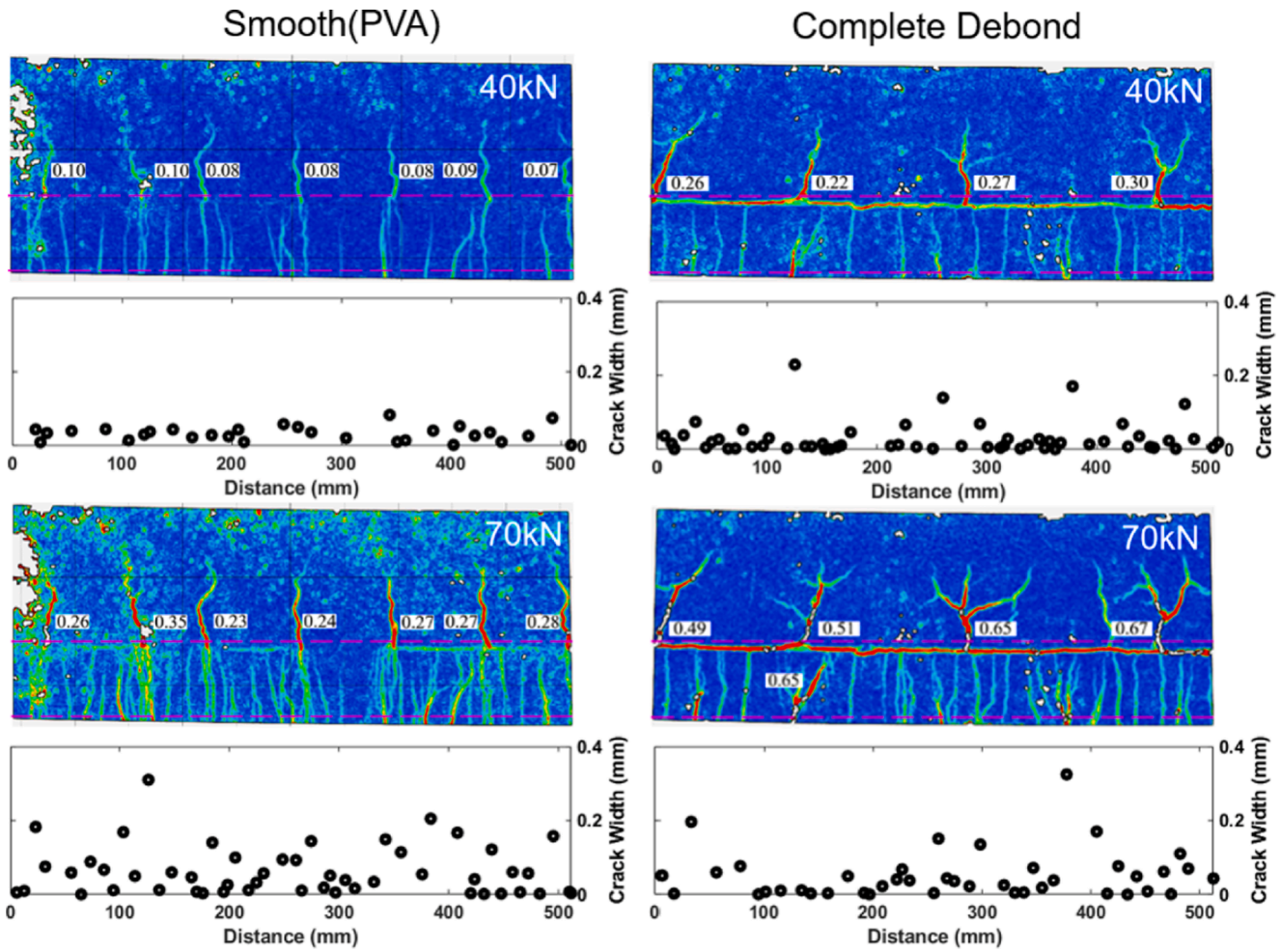

Fig. 11. Crack widths in SHCC and concrete for Smooth(PVA) and Complete Debond at 40 kN and 70 kN. The crack widths in concrete are labelled in the image while the crack widths in SHCC are shown as a scatter plot below the DIC plots.

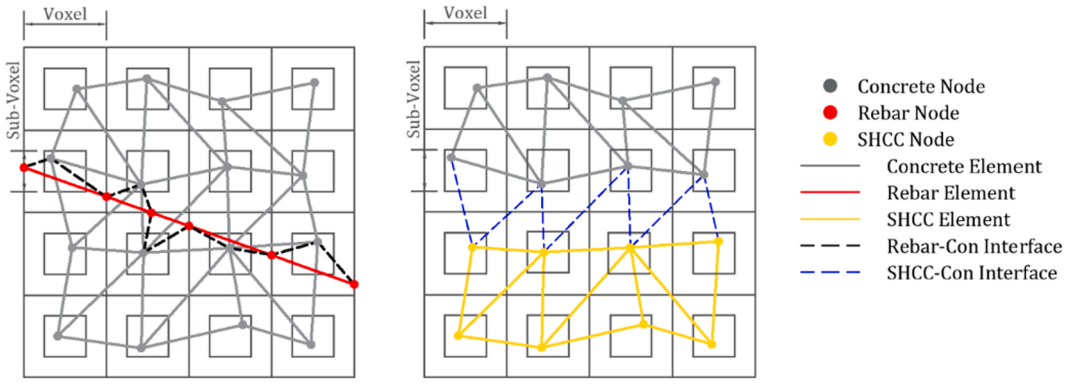

Fig. 12. 2D representation of generation of lattice mesh with (a) reinforcement and (b) interface.

- To simulate the interface, material distribution from beam geometry is overlapped on the lattice nodes. Two different type of nodes, SHCC and concrete are defined following the beam geometry (Fig. 2, Fig. 12 and Fig. 13). All the elements sharing the same type of node (concrete-concrete or SHCC-SHCC) are specified the corresponding properties of that material, while the element sharing two different types of nodes (concrete-SHCC or SHCC-concrete) are assigned interface properties and are referred to as SHCC-Con interface elements in Fig. 12.

Subsequently, the beams with different roughness profiles of the interface are generated (Fig. 13). The load is applied following the loading configuration of the experiments. Only the effective span of the beam is modelled. The results of the simulations are discussed for the region of interest, as labelled in Fig. 13. To avoid local damage around the loading and support plates, these "support" and "loading" elements are modelled such that they cannot break in tension or compression (coloured in red in Reinforced Concrete in Fig. 13).

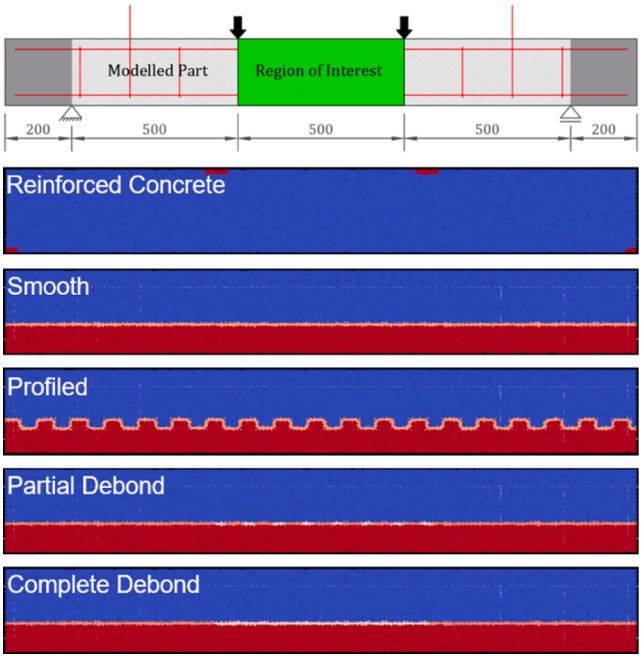

Fig. 13. Definition of the modelled part of the beams, region of interest for which numerical results are shown and lattice representation of the reference and hybrid beams. Blue (Concrete), Red (SHCC), Pink (Interface) and White (Debond).

4.2. Material definition

The lattice elements are assigned mechanical properties based on the materials they represent. The cross-sectional definition of the elements also influences the global response of the model. All the lattice elements are assumed to be cylindrical and have a circular cross-section. The radius of these elements is iteratively defined such that the global elastic modulus observed in the lattice simulation is equal to the input of elastic modulus for each element in a direct tension test. This ensures that the stiffness of the members is simulated appropriately.

In general, when modelling concrete with the lattice model, each element is assigned a stiffness and strength value. Since in these simulations the plasticity is introduced for some elements (e.g. reinforcement, the interface between steel and concrete), material properties for those elements are assigned as a list of values corresponding to the stiffness and strength. Each pair represents a point on the stress–strain curve of the material and is referred as a segment. For materials with more than one segments, when the stress in that element reaches its strength, the lattice elements loose the stiffness gradually by moving from one segment to the next rather than being completely removed from the mesh as in the case of one segment (brittle) materials.

The parameters in the lattice model are determined by inverse modelling, i.e. they are adjusted such that the response of the material tests and structural behaviour of reference (Reinforced Concrete) beam fit the experimental results. Concrete is simulated such that it has a compressive strength of 46 MPa in accordance with the experimental results. Tensile strength and elastic modulus of concrete are not tested, but are derived from compressive strength using analytical expressions provided by Eurocode [12] and are simulated accordingly.

The reinforcement is simulated as a bilinear hardening material with yield strength of 500 MPa and an ultimate strength of 550 MPa, following the characteristic properties of B500 steel used in the experiments. The ultimate strain capacity of the applied reinforcement is assumed to be 4.5% following the provisions of the Eurocode [12].

To simulate ductility for bond slip behaviour of reinforcement, the Rebar-Concrete interface elements are defined using seven segments as seen in Table 3. Similar elastoplastic definition of rebar-concrete bond is used in an earlier study [33]. The strength of interface elements is determined by fitting the simulated crack growth to the experimental observations for the reinforced concrete sample.

The direct tension response of simulated SHCC on a 100 mm × 100 mm × 200 mm prism is shown in Fig. 14. The maximum crack width in the figure corresponds to the widest crack in the simulation and the average crack width is the average of all the cracks along the height of SHCC. SHCC is defined using 3 segments such that the modelled SHCC exhibits good crack width control, where the maximum crack width in SHCC at ultimate strain level is below 50 microns (Fig. 14b). However, due to the used mesh size of 10 mm and the fact that only 1 crack can develop within this length, the simulated SHCC has much lower ductility (0.27%) compared to experiments (around 3% [21]). Crack spacing and crack widths govern the ductility of SHCC. In experiments, the cracks in SHCC develop with smaller spacing and lead to larger ductility. As the prediction of the maximum crack widths in SHCC is of interest in this study, and not necessarily the ductility, it is decided to proceed with the described modelling approach, with the note that it might underestimate the ductility of the simulated hybrid beams. The elastic modulus of SHCC is tested and accordingly used in the simulations.

In order to simplify the input for the SHCC-Con interface, the strength values are assigned equal to 50% of the concrete values while the stiffness is kept the same as that of concrete. For simulation of the hybrid beams with partial and complete debond, the debonded regions are assigned properties equivalent to 10% of the concrete properties. Table 3 shows the details of all the materials in reported simulations.

4.3. Numerical results

First, the results of the reference (Reinforced Concrete) sample are considered for verification of the model. This is necessary to determine (i.e. fit) the concrete-reinforcement bond properties such that the cracking behaviour and crack widths in simulated reference beam corresponds to the experimental observations. These properties are kept constant for all the remaining simulations. In Fig. 15, the load-deformation-maximum crack width response of tested and simulated reinforced concrete beam is compared. It can be seen that the selected modelling choices are able to simulate the load deformation response well in terms of ultimate load, deformation capacity and yielding of reinforcement. Equally important for the aims of this study, the simulated maximum crack widths are in good agreement when compared to experimental observations throughout the loading.

In Fig. 16, the development of damage in the lattice simulation and the total damage captured using DIC is compared at every 30 kN increase in the load. The lattice simulation is able to develop typical

Table 3
Input material properties for lattice simulations.

Material	E (GPa)	f_t (MPa)	f_c (MPa)
Concrete	32	4.00	$-17.5f_t$
SHCC	18.5	3.00	$-20f_t$
	9.25	3.75	$-20f_t$
	1.125	4.50	$-20f_t$
Concrete-SHCC Interface	32	2.00	$-17.5f_t$
Debonded interface	32	0.40	$-17.5f_t$
Rebar	200	500	$-f_t$
	12	550	$-f_t$
Rebar-Concrete Interface	32	3.25	$-10f_t$
	2	3.25	$-10f_t$
	1.5	3.25	$-10f_t$
	1.0	3.25	$-10f_t$
	0.75	3.25	$-10f_t$
	0.50	3.25	$-10f_t$
	0.40	3.25	$-10f_t$

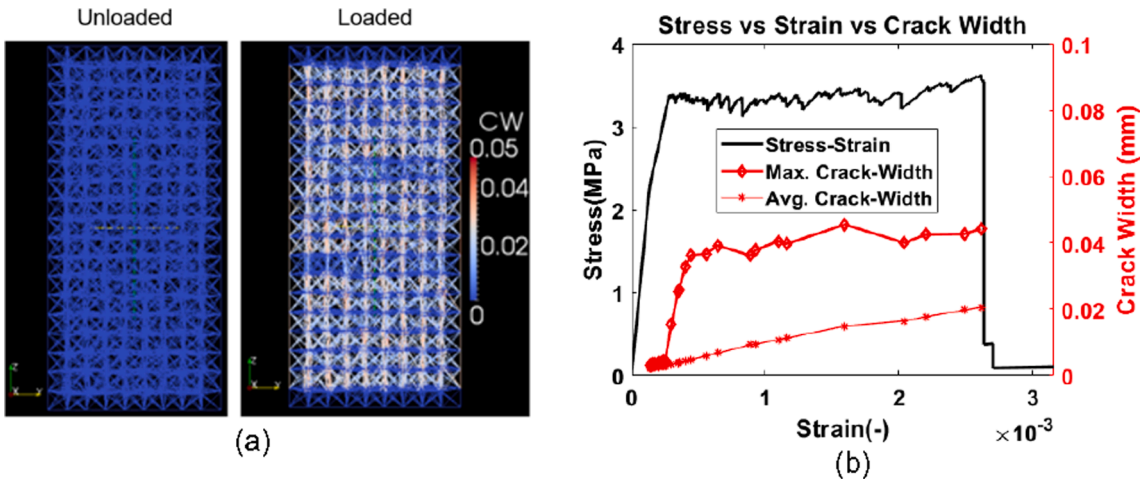

Fig. 14. (a) Unloaded and loaded sample in direct tension used for SHCC calibration – CW is crack width. (b) Stress-Strain response of simulated SHCC combined with the development of average and maximum crack widths until failure.

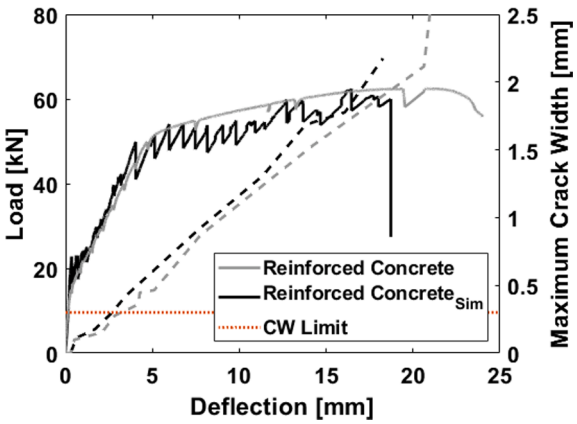

Fig. 15. Load-deformation-crack width response of tested and simulated reference beam.

flexural cracks, with accurate crack spacing in the constant moment region. The tilting of the cracks after reaching the compressive zone is also visible in both experimental and numerical results. From the results in Fig. 15 and Fig. 16, it can be seen that the selected modelling choices are able to simulate, in detail, the behaviour of Reinforced Concrete for the given boundary conditions. Therefore, the same approach is used in efforts to simulate the behaviour of hybrid beams.

Fig. 17a shows the result of simulated and tested hybrid (Smooth (PVA)) and reference (Reinforced Concrete) beam. Although the capacity and the contribution of SHCC to the increased capacity of the hybrid beams are reasonably captured, it can be seen that the simulated hybrid beam shows a significantly stiffer response compared to the experimental measurements. One reason for this difference may be the shrinkage, which is not considered in the current modelling approach. In reality, due to shrinkage of SHCC, the hybrid beam is already preloaded before application of mechanical load. Some cracks in the SHCC layer were visible before mechanical load was applied. Although shrinkage can play a role, its effect cannot be clearly seen from the experimental results comparing the difference between the hybrid beams and the reference beam. Another factor for the difference in stiffness may be the modelling approach of SHCC. The SHCC is mainly simulated to develop comparable crack widths for the given mesh size which underestimates the ductility, resulting in larger stiffness for modelled SHCC compared to the experimental one. Although for the purpose of the current study, this is not considered critical, further investigation on this aspect will be done in future. For this study, the crack widths in simulated SHCC layer are in a reasonably good agreement with the experimental observation. The predicted peak load, cracking pattern and the benefit of adding SHCC layer on the ultimate capacity of the beam are also appropriately captured. Therefore, with the observed limitation of the model in mind, its ability to simulate the effects of surface roughness and delamination is regarded to be appropriate and is therefore further investigated.

Fig. 17b shows the response of all the simulated hybrid beams. As designed and observed in the experiments, all the simulated hybrid beams show a similar load deformation response with comparable ultimate load capacities. All the simulated beams show maximum crack widths exceeding 0.3 mm only after the ultimate failure of the beam, irrespective of the surface preparation. From the simulation analysis, the failure occurs once the strain capacity of SHCC is reached, after which the SHCC is not active to take further tensile loads and the beam fails. This is different compared to the experimental observations. In experiments, first the reinforcement yields then the cracks in SHCC exceed 0.3 mm limit and finally the beam fails. In addition, the deformation capacity of the simulated hybrid beam is lower when compared to the experiments. This is expected because of the low strain capacity of SHCC, which causes premature failure in simulation.

Even with this initial modelling approach limitations, the model is able to predict the final cracking pattern. Comparing the results in Fig. 18, it can be seen that the model is able to simulate the effect of varying interfacial treatment on the number of cracks developed in concrete. Furthermore, the damage at the interface for varying interfacial treatment is also well predicted with maximum opening for the Complete Debond followed by Smooth(PVA).

Note that the relationship between the lattice input parameters and simulated macroscopic properties is reported to be mesh size dependent [35] and is subjected to some scatter. However, by ensuring that the inverse analysis procedure is systematically imbedded throughout the modelling (i.e. starting from material simulation then flexural response of the reference sample and finally the hybrid beams) and that multiple performance criteria are compared for each test (e.g. load displacement curve, crack spacing and crack widths), the modelled parameters are considered to be robustly presented – especially given the limited number of the lattice parameters.

5. Discussion

From this experimental and numerical study, it is observed that the interfacial treatment in hybrid SHCC concrete structures exhibits an interplay between two effects leading to crack localization in SHCC. Where a weak bond is required to encourage the delamination of the

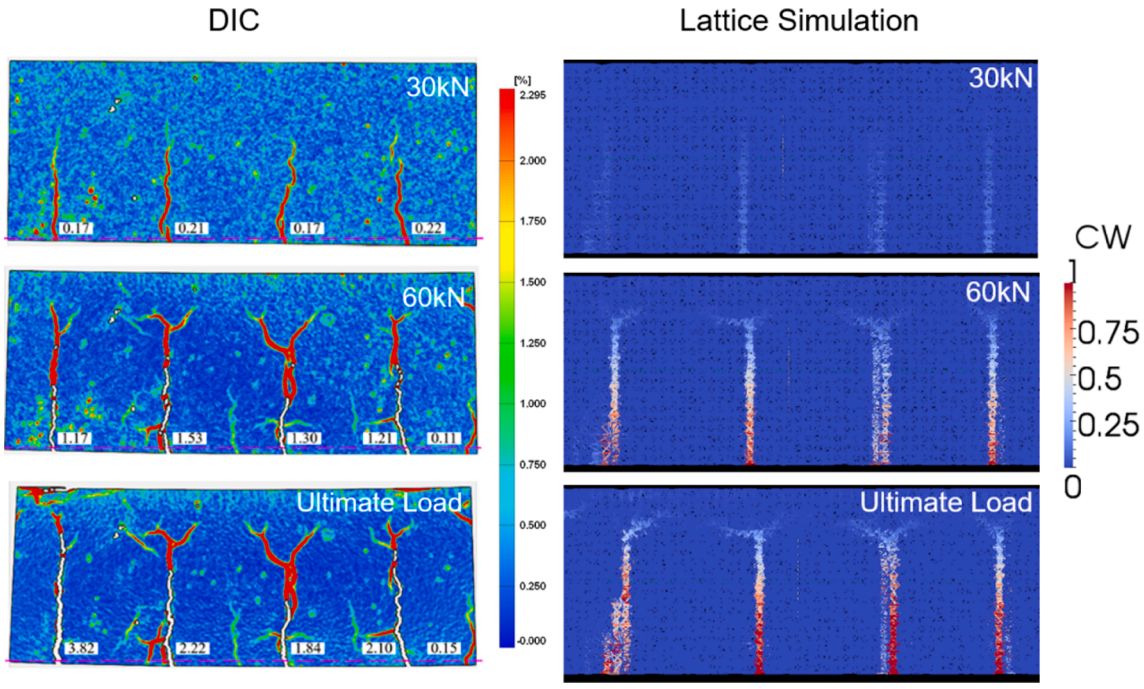

Fig. 16. Damage observed with DIC and lattice simulation at 30 kN, 60 kN and ultimate load. The experimental damage is represented by equivalent von Mises strain in DIC [29] and accompanied crack widths at the surface, whereas in the lattice model crack widths are presented.

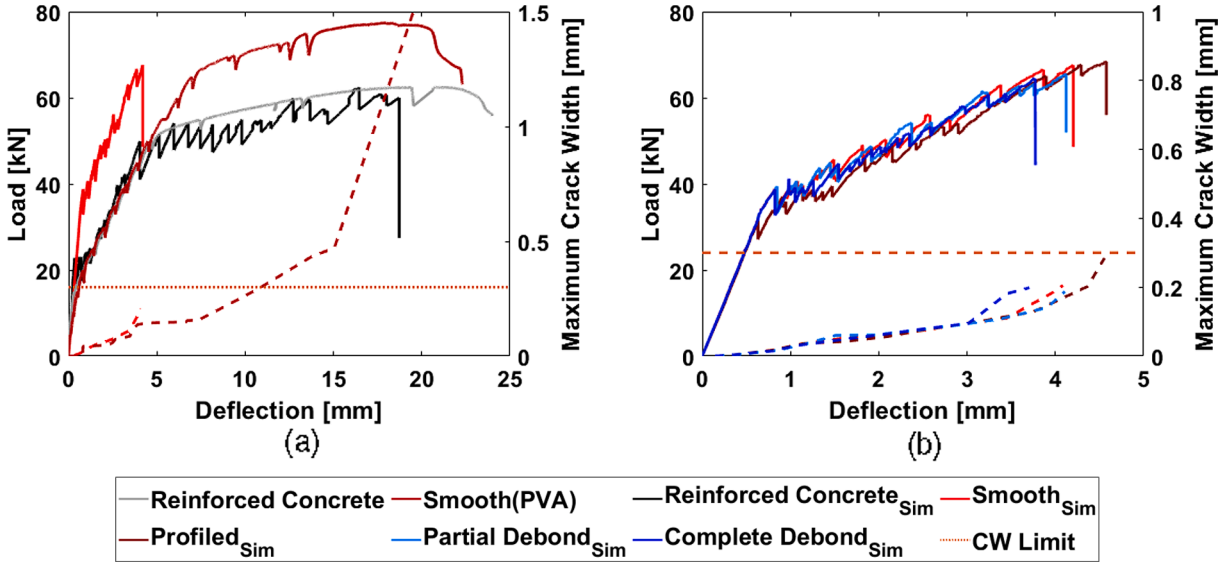

Fig. 17. (a) Numerical and experimental response of Reinforced Concrete and Smooth(PVA). (b) Numerical response of all the hybrid beams.

interface and activation of a larger portion of SHCC after cracking in concrete, a strong bond is required to ensure that SHCC acts as effective reinforcement in the hybrid configuration, also limiting the development of cracks. This is observed when comparing DIC images of Smooth (PVA) and Complete Debond: Smooth(PVA) exhibits linear cracks (uniform – almost constant strain) in SHCC while Complete Debond exhibits flexural cracks (linearly varying strain). To demonstrate this, the results of DIC are also presented using an alternate approach that highlights the crack development along the height of the beam. The envelopes of strain in x-direction (ε_{xx}) for both the beams at 50 kN using the same contour range and magnification are plotted in Fig. 19. It can be seen that at the same load, the composite action in Smooth(PVA) results in lower strains in concrete and SHCC when compared to Complete Debond. Since the SHCC in Complete Debond experiences larger strains at the same load, the cracks also localize at a lower load. The composite action can also be deduced from these plots. While, in Complete Debond there is a clear jump of strains at the interface, in Smooth (PVA), the strains at the interface are almost equal in concrete and SHCC. For structural behaviour of SHCC concrete hybrid beams, the action of SHCC as effective reinforcement of the concrete is the governing mechanism in crack width control. Therefore, a stronger interface is able to limit the crack widths until higher loads.

Acknowledging the limitations of the lattice model to simulate SHCC behaviour and the interface between SHCC and concrete, an attempt is made to confirm this trend numerically by comparing the crack development in concrete. Fig. 20 provides a comparison between experimental and numerically predicted maximum crack widths in the concrete part during the loading of the hybrid beams. All the models are

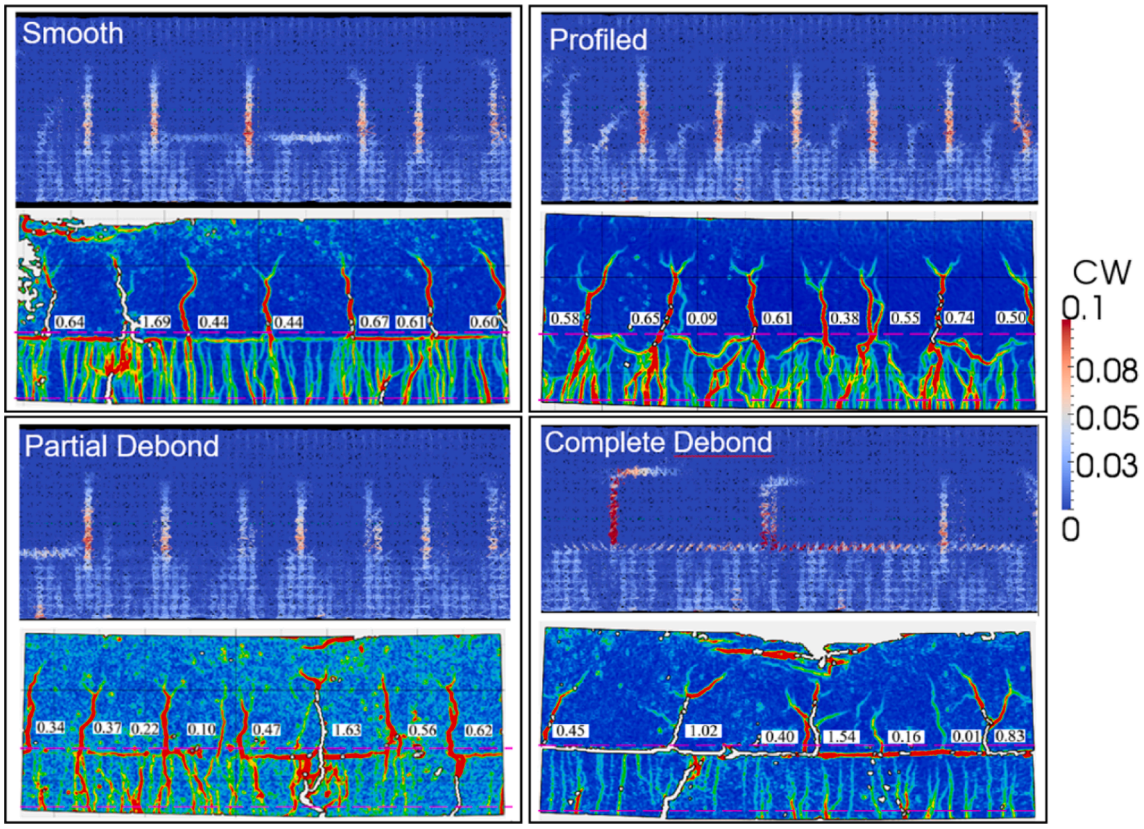

Fig. 18. Numerically obtained damage at the ultimate load for the hybrid beams compared to the experiments, with the legend for the numerically observed crack widths.

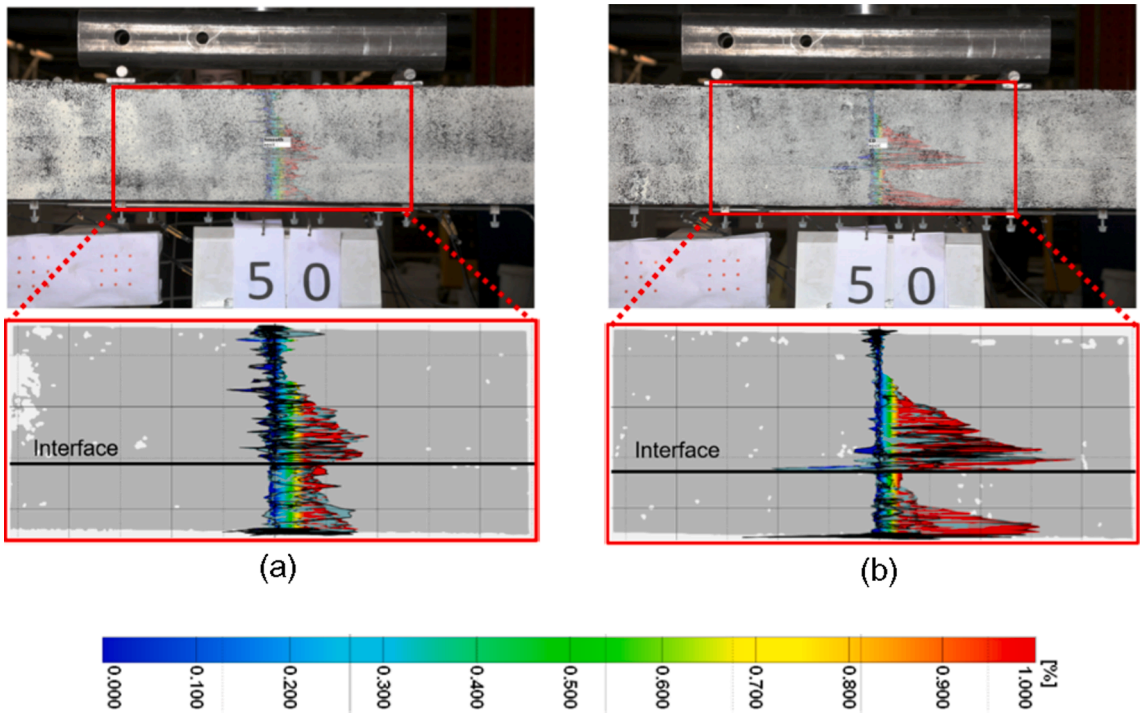

Fig. 19. The envelope of strain in x-direction for (a) Smooth(PVA) and (b) Complete Debond at 50 kN plotted at the mid-section of the DIC region.

able to predict the trend of maximum cracks in the concrete layer in reasonably good accordance with the experiments. The strong interface (Smooth(PVA) and Profiled) are able to realize the composite action between SHCC and concrete. Thus, SHCC is able to effectively reinforce the concrete part and limits the crack widths in the concrete. As the interface is weakened (Partial Debond and Complete Debond), the

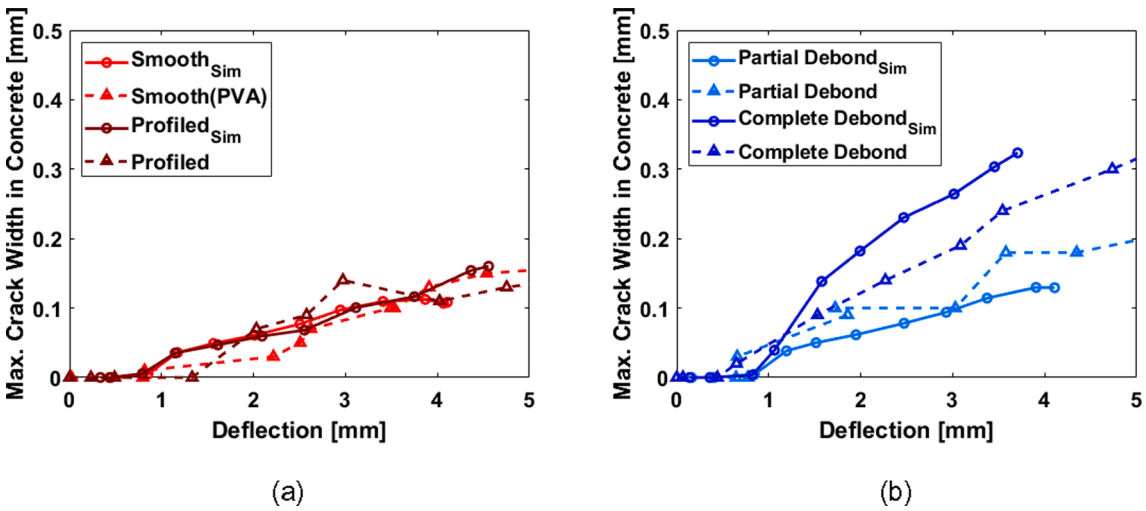

Fig. 20. Experimental and numerical maximum crack widths in concrete of hybrid beams in (a) Smooth(PVA) and Profiled and (b) Partial Debond and Complete Debond.

composite action is reduced and the cracks in concrete grow larger at lower deformations. This reinforces the initial claim that for new hybrid structures, the realization of composite action is the governing phenomenon for crack width control in both SHCC and concrete part of the beams.

It is realized that, besides the bond between concrete and SHCC, the type of reinforcement (smooth or ribbed) and the bond between reinforcement and SHCC, the reinforcement diameter and percentage, and the cover depth might also play a significant role on the crack width control and deformation capacity of the hybrid beams [36–40]. Especially the post-yielding ductility of (hybrid) fibre-reinforced concrete beams with ribbed rebars and strong bond is reported to be reduced compared to conventional reinforced concrete beams [36,37,39]. Although ribbed reinforcements were used in the current experiments, no reduction in ductility of hybrid beams was observed compared to the reference sample. The ductility and crack width development of such a hybrid system might be effected when higher reinforcement ratios or lower cover depths are used. Investigating the role of these parameters will be considered in future.

6. Conclusion

A combined experimental and numerical study is performed to investigate the role of the interface between SHCC and concrete, and the fibres applied in the SHCC on the crack width control ability of the hybrid SHCC concrete beams. The following conclusions can be drawn:

- Provision of 70 mm thick SHCC layer, with smooth interface, on the tension side of a 200 mm flexural member is confirmed to be effective in providing appropriate crack width control such that the SLS criterion is no longer governing for reinforcement design i.e., the cracks exceed the SLS limit after the yielding of longitudinal reinforcement.
- For the given assessment criterion of limiting the crack widths below 0.3 mm in SHCC, the replacement of PVA fibres with HMPE fibres did not result in further improvement in crack width control. However, for both the fibre types, the cracks in SHCC exceed this limit after the yielding of the reinforcement.
- The interface treatment between SHCC and concrete significantly influences the crack width control of hybrid beams. On the one hand, a stronger interface provides a more effective reinforcement of the concrete and therefore results in larger number and lower spacing of cracks in concrete, in turn resulting in lower crack width on the surface of SHCC. On the other hand, a strong interface causes more restraint and leads to early crack localization in the SHCC. The former is shown to be the governing mechanism in hybrid SHCC concrete systems. From DIC, it is observed that a stronger bond between SHCC and concrete assures that the SHCC is loaded rather uniformly, in tension. Contrarily, with no bond, SHCC predominantly experiences bending, leading to earlier crack localization. Thus, improving the bond between concrete and SHCC provides better crack width control, i.e. crack widths at the surface of SHCC exceed the 0.3 mm limit at higher loads.
- With relatively simple inputs of the interface, the lattice model is found to be promising in predicting and gaining insight into fracture behaviour of the hybrid systems. It can accurately simulate the crack development, peak load, crack distribution and final crack pattern. However, the failure mode is not properly captured. The stiffness of the hybrid beams is over predicted and deformation capacity is under predicted. The latter is possibly caused by the mesh size limitation and intrinsic microcracking behaviour of SHCC, where crack spacing in reality is much smaller than in the model. Further research is required to develop a modelling approach, which captures both, the crack width control and the deformation capacity of the hybrid beams.

CRediT authorship contribution statement

Shozab Mustafa: Data curation, Formal analysis, Investigation, Methodology, Software, Writing – original draft, Visualization. **Shantanu Singh:** Data curation, Formal analysis, Investigation, Methodology. **Dick Hordijk:** Conceptualization, Writing – review & editing. **Erik Schlangen:** Project administration, Supervision, Validation, Writing – review & editing. **Mladena Luković:** Conceptualization, Funding acquisition, Project administration, Methodology, Resources, Supervision, Validation, Writing – review & editing.

Declaration of Competing Interest

The authors declare that they have no known competing financial interests or personal relationships that could have appeared to influence the work reported in this paper.

Acknowledgements

This work was supported by the Dutch Organization for Scientific Research (NWO) under the grant “Optimization of interface behaviour

for innovative hybrid concrete structures" (project number 16814).

Data availability

The raw data required to reproduce the load-deformation response and the processed data to reproduce the crack width response of the beams are available to download from [DOI: 10.4121/14672064].

References

[1] Hordijk DA. Local approach to fatigue on concrete. PhD Dissertation. Delft University of Technology; 1991.

[2] Li VC, Wang S, Wu C. Tensile strain-hardening behavior or polyvinyl alcohol engineered cementitious composite (PVA-ECC). ACI Mater J 2001;98:483–92. https://doi.org/10.14359/10851.

[3] Lin Z, Li VC. Crack bridging in fiber reinforced cementitious composites with slip-hardening interfaces. J Mech Phys Solids 1997;45(5):763–87. https://doi.org/10.1016/S0022-5096(96)00095-6.

[4] Van Zijl GPAG, Slowik V. A Framework for Durability Design with Strain-Hardening Cement-Based Composites (SHCC). State-of-the-Art RILEM Rep 2017; 22. https://doi.org/10.1007/978-94-024-1013-6.

[5] Wang G, Yang C, Pan Y, Zhu F, Jin K, Li K, et al. Shear Behaviors of RC Beams Externally Strengthened with Engineered Cementitious 2019.

[6] Zhang Y, Bai S, Zhang Q, xie H, Zhang X. Failure behavior of strain hardening cementitious composites for shear strengthening RC member. Constr Build Mater 2015;78:470–3. https://doi.org/10.1016/j.conbuildmat.2015.01.037.

[7] Khalil AE, Etman E, Atta A, Essam M. Behavior of RC beams strengthened with strain hardening cementitious composites (SHCC) subjected to monotonic and repeated loads. Eng Struct 2017;140:151–63. https://doi.org/10.1016/j.engstruct.2017.02.049.

[8] Shang X, Yu J, Li L, Lu Z. Strengthening of RC Structures by Using Engineered Cementitious Composites : A Review 2019.

[9] Li Q, Xu S. Experimental investigation and analysis on flexural performance of functionally graded composite beam crack-controlled by ultrahigh toughness cementitious composites. Sci China, Ser E Technol Sci 2009;52(6):1648–64. https://doi.org/10.1007/s11431-009-0161-x.

[10] Luković M, Huang Z, Hordijk DA, Schlangen E. Strain Hardening Cementitious Composite (SHCC) for crack width control in reinforced concrete beams. Heron 2019;64:189–206.

[11] Randl N. Design recommendations for interface shear transfer in fib Model Code 2010. Struct Concr 2013;14(3):230–41. https://doi.org/10.1002/(ISSN)1751-764810.1002/suco.v14.310.1002/suco.201300003.

[12] 1992-1-1 E. EN 1992-1-1 Eurocode 2 - Design of concrete structures - Part 1-1: General rules and rules for buildings. vol. 1. 2011.

[13] Júlio ENBS, Branco FAB, Silva VD, Lourenço JF. Influence of added concrete compressive strength on adhesion to an existing concrete substrate. Build Environ 2006;41(12):1934–9. https://doi.org/10.1016/j.buildenv.2005.06.023.

[14] Luković M, Schlangen E, Ye G, Šavija B. Impact of surface roughness on the debonding mechanism in concrete repairs. In: Proc 8th Int Conf Fract Mech Concr Concr Struct Fram 2013; 2013. p. 611–21.

[15] Luković M. Influence of interface and strain hardening cementitious composites (SHCC) properties on the performance of concrete repairs. 2016.

[16] Kunieda M, Kamada T, Rokugo K, Bolander JE. Localized fracture of repair material in patch repair systems. Proc Fram 2004.

[17] Kamada T, Li VC. Effects of surface preparation on the fracture behavior of ECC/concrete repair system. Cem Concr Compos 2000;22:423–31. https://doi.org/10.1016/S0958-9465(00)00042-1.

[18] Li VC. Engineered Cementitious Composites (ECC) Bendable Concrete for Sustainable and Resilient Infrastructure. Michigan, USA: Springer; 2019.

[19] Savino V, Lanzoni L, Tarantino AM, Viviani M. A cohesive FE model for simulating the cracking/debonding pattern of composite NSC-HPFRC/UHPFRC members. Constr Build Mater 2020;258:119516. https://doi.org/10.1016/j.conbuildmat.2020.119516.

[20] Sadouki H, Denarié E, Brühwiler E. Validation of a FEA model of structural response of RC-cantilever beams strengthened with a (R-) UHPFRC layer. Constr Build Mater 2017;140:100–8. https://doi.org/10.1016/j.conbuildmat.2017.02.090.

[21] Zhou J. Performance of Engineered Cementitious Composites for Concrete Repairs. 2011.

[22] 12390-3 N-E. NEN-EN 12390-3 Testing hardened concrete - Part 3: Compressive strength of test specimens. 2017.

[23] McCormick N, Lord J. Digital image correlation. Mater Today 2010;13(12):52–4. https://doi.org/10.1016/S1369-7021(10)70235-2.

[24] Schindelin J, Arganda-Carreras I, Frise E, Kaynig V, Longair M, Pietzsch T, et al. Fiji: An open-source platform for biological-image analysis. Nat Methods 2012;9(7):676–82. https://doi.org/10.1038/nmeth.2019.

[25] Mustafa S, Singh S, Luković M. Effect of interface treatment on the cracking behaviour of hybrid SHCC (strain hardening cementitious composite) concrete beams. In: Bin Zhao and Xilin Lu, editor. fib Symp. 2020, Concr. Struct. Resilient Soc., Shanghai, China: federation internationale du beton (fib) – Internation Federation for Structural Concrete; 2020, p. 456–62.

[26] Gehri N, Mata-Falcón J, Kaufmann W. Automated crack detection and measurement based on digital image correlation. Constr Build Mater 2020;256:119383. https://doi.org/10.1016/j.conbuildmat.2020.119383.

[27] Ghorbani R, Matta F, Sutton MA. Full-field deformation measurement and crack mapping on confined masonry walls using digital image correlation. Exp Mech 2015;55(1):227–43. https://doi.org/10.1007/s11340-014-9906-y.

[28] Tung S-H, Shih M-H, Sung W-P. Development of digital image correlation method to analyse crack variations of masonry wall. Sadhana – Acad Proc Eng Sci 2008;33(6):767–79. https://doi.org/10.1007/s12046-008-0033-2.

[29] Shih MH, Sung WP. Application of digital image correlation method for analysing crack variation of reinforced concrete beams. Sadhana - Acad Proc Eng Sci 2013;38(4):723–41. https://doi.org/10.1007/s12046-013-0141-5.

[30] Yip M, Mohle J, Bolander JE. Automated modeling of three-dimensional structural components using irregular lattices. Comput Civ Infrastruct Eng 2005;20(6):393–407. https://doi.org/10.1111/mice:2005.20.issue-610.1111/j.1467-8667.2005.00407.x.

[31] Schlangen E, Garboczi EJ. Fracture simulations of concrete using lattice models: computational aspects 1997;57:319–32.

[32] Šavija B, Luković M, Schlangen E. Influence of cracking on moisture uptake in strain-hardening cementitious composites. J Nanomech Micromech 2017;7:1–8. https://doi.org/10.1061/(ASCE)NM.2153-5477.0000114.

[33] Lukovic M, Yang Y, Schlangen E, Hordijk D. On the Potential of Lattice Type Model for Predicting Shear Capacity of Reinforced Concrete and SHCC Structures. High Tech Concr Where Technol Eng Meet 2018;1:804–13. https://doi.org/10.1007/978-3-319-59471-2_94.

[34] Pan Y, Prado A, Porras R, Hafez OM, Bolander JE. Lattice modeling of early-age behavior of structural concrete. Materials (Basel) 2017;10:1–34. https://doi.org/10.3390/ma10030231.

[35] Delaplace A, Desmorat R. Discrete 3D model as complimentary numerical testing for anisotropic damage. Int J Fract 2007;148(2):115–28. https://doi.org/10.1007/s10704-008-9183-9.

[36] Schumacher P. Rotation capacity of self-compacting steel fiber reinforced concrete. 2006.

[37] Oesterlee C. Structural Response of Reinforced UHPFRC and RC Composite Members 2010:159. https://doi.org/10.5075/epfl-thesis-4848.

[38] Moreno DM, Trono W, Jen G, Ostertag C, Billington SL. Tension stiffening in reinforced high performance fiber reinforced cement-based composites. Cem Concr Compos 2014;50:36–46. https://doi.org/10.1016/j.cemconcomp.2014.03.004.

[39] Bandelt MJ, Billington SL. Simulating bond-slip effects in high-performance fiber-reinforced cement based composites under cyclic loads. In: Comput Model Concr Struct - Proc EURO-C 2014, 2; 2014. p. 1059–66. https://doi.org/10.1201/b16645-117.

[40] Shao Yi, Billington SL. Flexural performance of steel-reinforced engineered cementitious composites with different reinforcing ratios and steel types. Constr Build Mater 2020;231:117159. https://doi.org/10.1016/j.conbuildmat.2019.117159.